ACS APPLIED MATERIALS & INTERFACES

Research Article

www.acsami.org

Uniform Graphitic Carbon Nitride Nanorod for Efficient Photocatalytic Hydrogen Evolution and Sustained Photoenzymatic Catalysis

Jian Liu,*[,†] Jianhui Huang,*[,‡] Han Zhou,[†,#] and Markus Antonietti[†]

[†]Department of Colloid Chemistry, Max Planck Institute of Colloids and Interfaces, 14424 Potsdam, Germany

[‡]College of Environmental and Biological Engineering, Putian University, Putian 351100, P. R. China

[#]State Key Lab of Metal Matrix Composites, Shanghai Jiaotong University, Shanghai 200240, P. R. China

Supporting Information

ABSTRACT: Uniform graphitic carbon nitride nanorods (CNR) were facilely obtained by a morphology-preserving strategy by templating a chiral mesostructured silica nanorod. The hexagonal mesostructured pore structures of one-dimensional silica nanorods can provide nanoconfinement space for carbon nitride condensation to perfect layered structures. CNR demonstrated excellent photocatalytic capability in generating hydrogen from water even with a small specific surface area, compared with its mesoporous counterpart. For further application demonstration, the CNR was used for photocatalytic regeneration of NAD^+ to NADH, the biological form of hydrogen. The in situ NADH regeneration system was further coupled with L-glutamate dehydrogenase for sustainable generation of L-glutamate from α-ketoglutarate. The high yield and high efficiency obtained here point a high-throughput and sustainable way for practical enzymatic applications.

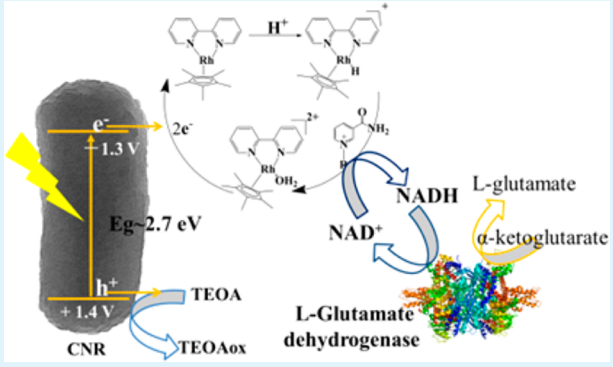

KEYWORDS: *graphitic carbon nitride, morphology-preserving, nanorod, photocatalytic, enzymatic, NADH regeneration*

INTRODUCTION

In natural photosynthesis, chlorophyll molecules were excited by light energy, with photoinduced electrons passing through an electron transport chain to reduce nicotinamide adenine dinucleotide phosphate (NAD(P)) to NAD(P)H, completing the storage of light energy.[1] The chlorophyll molecule then regains the lost electron from water through a photolysis process, which releases a dioxygen molecule. In the light-independent reaction, with the newly formed NAD(P)H, the specific enzyme captures and converts CO_2 into three-carbon sugars, which are later combined to form sucrose and starch. All the photosynthetic reactions are catalyzed by enzyme. Enzymes are long recognized as extremely efficient and mild catalysts in scientific and industrial activities. Inspired by natural photosynthesis, artificial photosynthesis involves the solar-to-chemical energy conversion processes including water splitting, CO_2 reduction and some light-mediated enzymatic reactions.[2−4] To accomplish the practical artificial photosynthesis, it is highly challenging but desirable to develop an efficient system that can perform multiple tasks toward artificial photosynthesis.[5,6] Therefore, facile synthesis of high efficiency multifunctional systems for light energy conversion is crucial for realizing practical artificial photosynthesis.[2,5,7]

Graphitic carbon nitride materials have gained intense interests of the scientific community because of their unique and excellent properties in thermal and chemical stability. Specially, graphitic carbon nitride is in the focus due to the recently disclosed visible-light-driven photocatalytic properties.[8,9] The appropriate bandgap width and easy engineering properties for extending the absorbance spectrum render g-C_3N_4 very popular and promising in such field.[10−13] Therefore, various templates have been proposed acting as the structure directing agents for the desired carbon nitride nanostructures, including biological materials, Anodic Aluminum Oxide membrane, and various SiO_2-based nanostructures et al.[14−16] However, considering the cost and complicated procedures in obtaining/combining with previous templates, facile fabrication of uniform nanostructured g-C_3N_4 with high photocatalytic efficiency is still a big issue toward the practical application purposes.

Herein, the uniform graphitic carbon nitride nanorods (CNR) were facilely synthesized by templating from monodisperse, chiral mesostructured silica nanorods (MSR), which were easily fabricated through ammonia-catalyzed hydrolysis of tetraethyl orthosilicate by using binary F127 and CTAB as templates.[17] The obtained one-dimensional CNR was com-

Received: March 5, 2014
Accepted: May 6, 2014
Published: May 6, 2014

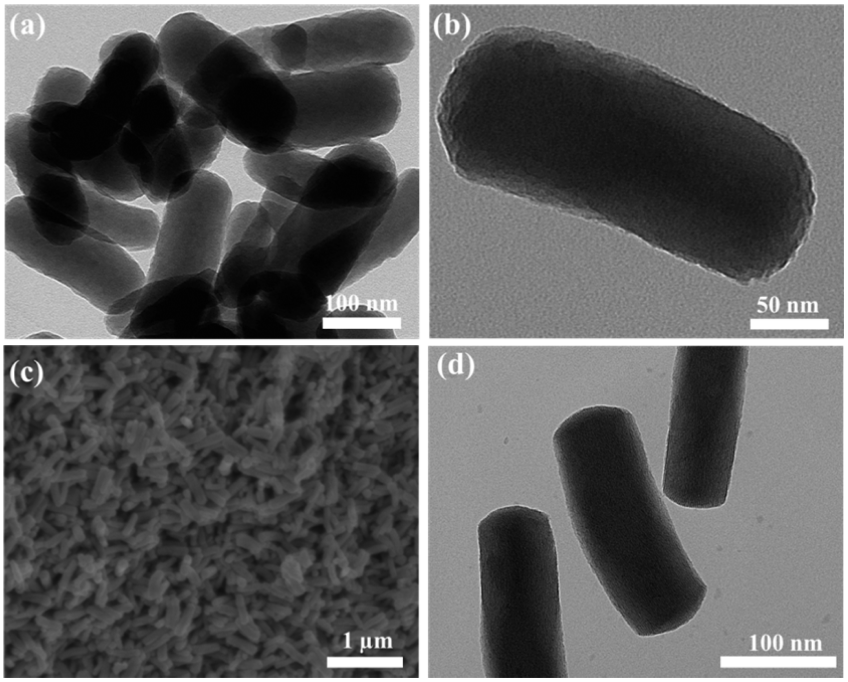

Figure 1. (a) TEM image of CNRs. (b) TEM image of a single CNR, featuring the nanosheet as the building block. (c) SEM image of large area overview, illustrating the uniform and monodisperse properties of CNRs. (d) TEM image of chiral mesostructured SiO_2 nanorod.

posed with layered carbon nitride sheets. Pt nanoparticles decorated CNR (Pt@CNR) demonstrated surprisingly high photocatalytic activity in hydrogen evolution from water in the presence of triethanolamine even comparing with mesoporous counterpart. The enhancement is ascribed to the highly efficient charge separation efficiency in the one-dimensional nanorod. Furthermore, CNR was employed for photocatalytic regeneration of coenzyme NADH, a substance essential for enzymes to gain full functionality.[18−20] The NADH regeneration system was coupled with the L-glutamate dehydrogenase for sustainable synthesis of chiral L-glutamate from α-ketoglutarate.[21−23] Stoichiometric enzymatic catalysis of α-ketoglutarate to L-glutamate was accomplished in the presence of in situ NADH regeneration system by CNR photocatalysis. The work reported here could provide a feasible method to construct high efficiency artificial light energy conversion systems and also an excellent building block for further facilitated engineering and assembly into periodic array for artificial photosynthetic device in the near future.

EXPERIMENTAL SECTION

Materials. Cyanamide, triethanolamine (TEOA), rhodium(III) chloride hydrate, 2,2′-bipyridyl, 1,2,3,4,5-pentamethylcyclopentadiene, and β-nicotinamide adenine dinucleotide phosphate sodium salt hydrate (β-NAD^+), α-ketoglutarate, and L-glutamate dehydrogenase (GDH) were purchased from Sigma-Aldrich.

Synthesis of CNR. The synthesis of chiral mesostructured silica nanorods was simply achieved by using F127 and CTAB as binary templates in basic aqueous solutions at room temperature. Typically, F127 (0.123 g), H_2O (3.5 mL), CTAB (12.5 mL, 0.04 M), and aqueous ammonia solution (15 mL, 2.5 wt %) were mixed to form a clear solution, to which TEOS (0.6 mL) was added under stirring. After 2 min of stirring, the mixture was allowed to stand under static conditions at room temperature for 3 h, leading to the formation of a white suspension. The SiO_2 nanorod was obtained after centrifugation followed by drying and calcination to remove the organic substance.

A mixture of 1 g of as-calcined SiO_2 nanorod and 5 g of cyanamide was degassed for 3 h followed by sonication in water for 2 h. After remove surplus cyanamide by water dissolving, the obtained white solid was transferred to a crucible with lid and heated under air at 2.3 °C min^{-1} up to 550 °C (4 h) and kept at 550 °C for another 4 h. The resultant yellow powder is treated with 4 M NH_4HF_2 solution for 48 h. The dispersion is then filtered and the yellow precipitate is copiously rinsed with deionized water and ethanol. Finally, the yellow powder is dried under vacuum at 60 °C overnight.

mpg-C_3N_4 was Synthesized As Follows. Five grams of cyanamide and 12.5 g of Ludox-HS 40 colloidal silica suspension (1:1of solid ratio) are mixed together until the complete dissolution of cyanamide. The other procedure is the same as CNR. g-C_3N_4 was obtained through the thermal condensation of cyanamide at 550 °C (4 h) under air and used as second control sample.

$[Cp^*Rh(bpy)H_2O]^{2+}$ was Synthesized As Follows. $RhCl_3{\cdot}H_2O$ is refluxed in methanol with one equivalent of 1,2,3,4,5-pentamethylcyclopentadiene for 24 h. The resulting red precipitate is filtrated and suspended in methanol. On addition of two equivalents of 2,2-bipyridine, the suspension clears up immediately and a yellowish solution is formed. [Cp*Rh(bpy)Cl]Cl is precipitated on the addition of diethyl ether into the obtained yellowish solution. Stock solutions (100 mM) are prepared in water and stored at room temperature avoiding direct light exposure. [Cp*Rh(bpy)Cl]Cl readily hydrolyzes to $[Cp^*Rh(bpy)(H_2O)]^{2+}$.

Characterization. XRD measurements were performed on a D8 Diffractometer from Bruker instruments (Cu Kα radiation, λ = 0.154 nm) equipped with a scintillation counter. N_2 sorption experiments were done with a Quantachrome Autosorb-1 at liquid nitrogen temperature. TEM images were taken on Philips CM200 FEG (Field Emission Gun), operated at an acceleration voltage of 200 kV. SEM measurement was performed on a LEO 1550 Gemini instrument. The UV−vis absorbance spectra were recorded on a T70 UV/vis spectrophotometer. The FTIR spectrum was collected using a Varian 1000 FTIR spectrometer.

NADH Regeneration. In a typical regeneration procedure, the reaction medium was composed of NAD^+ (1 mM), TEOA (15 w/v%), phosphate buffer (100 mM) and 3 mg of carbon nitride materials. The pH value of the reaction media were set to 8 for mediator involved system. The reaction system was placed into a degassed quartz reactor equipped with stirring bar and illuminated with white LED lamp. The distance between reactor and LED lamp is fixed at 15 cm. During the

dx.doi.org/10.1021/am501319v | ACS Appl. Mater. Interfaces 2014, 6, 8434−8440

illumination, the concentration of NADH was estimated by measuring the absorbance of diluted reaction system at 340 nm. NAD^+ has peak absorption at a wavelength of 260 nm, with an extinction coefficient of 16 900 M^{-1} cm^{-1}. NADH has peak absorption at 340 nm with an extinction coefficient of 6,220 M^{-1} cm^{-1}.

Photoenzymatic Reaction. The reaction medium for the photoenzymatic synthesis of L-glutamate includes NAD^+ (1 mM), **M** (0.5 mM), α-ketoglutarate(10 mM), $(NH_4)_2SO_4$ (100 mM), GDH (40 U), 0.1 M pH 7.4 phosphate buffer with 15 w/v% of TEOA, and 3 mg of CNR. The reaction solution was stirred in the dark for 1 h followed by 8 h continuous light reaction.

RESULTS AND DISCUSSION

The CNR was obtained through templating a mesostructured SiO_2 nanorod (MSR) (see Figure S1 in the Supporting Information, SI), which was synthesized using F127 and CTAB as binary templates. The MSRs exhibit a slightly twisted chiral structure, which is thought to be shape-controlling role of F127 played in the formation process while CTAB mainly contributed to the pore structure of MSRs.[17] The loading of cyanamide precursor into the MSR is the key point in successfully fabricating the CNR. Reduced reactor pressure under elevated temperature above melting point of cyanamide (47 °C) greatly facilitated infiltration process. The nonporous carbon nitride/MSR composite nanorod was illustrated in Figure S2 in the Supporting Information, indicating the good infiltration of precursor in the confined nanospace. The schematic fabrication process of CNR was schematically illustrated in Scheme S1 of the Supporting Information.

TEM image in Figure 1a demonstrates that the obtained CNR was with size of 200 nm long and 80 nm wide. Looking into the detail in Figure 1b gives the clue that the nanorod is composed of layered carbon nitride sheet, which can be clearly observed from the edges of CNR. The control experiments were performed to shed some light on the formation mechanism of CNR featuring layer carbon nitride as building blocks (see Figures S3–S5 in the Supporting Information, respectively).

As illustrated in Figure 1c, the CNR demonstrated the uniform and monodisperse properties over large area view. TGA analysis (see Figure S6 in the Supporting Information) demonstrates that 5% of silica residue was found to left in the final CNR samples, indicating most of the silica template was successfully removed during the etching process.

Surprisingly, templating from a MSR turns out to be nonporous CNR with nanosheet as building block. The collapse of the mesostructure is presumably ascribed to the overfilling of molten cyanamide in the interior of template and large shrinkage during the high-temperature condensation.[24] The texture and structure of the CNR, mesoporous CN, and bulk CN samples were characterized by nitrogen adsorption–desorption measurements. The isotherms and the Barrett–Joyner–Halenda (BJH) pore size distributions are shown in Figure 2. The isotherms of mesoporous CN show typical hysteresis, proving the existence of larger mesopores connected via micropores, whereas for the CNR and bulk CN samples, the adsorption and desorption isotherms almost coincide, indicating the lack of mesoporous structure. The difference in pore structure leads to their significant difference in BET surface areas: the BET surface area of CNR is 52 m^2/g, and its 25 m^2/g for bulk CN, which is much smaller than the 230 m^2/g for mesoporous CN. Comparing with the previously reported results, the liquid phase infiltration of cyanamide aqueous solution into the mesostructured template will lead to

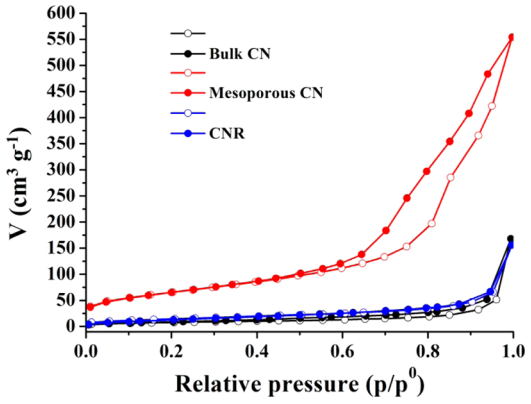

Figure 2. N_2 sorption–desorption isotherms of CNR, mesoporous CN, and bulky CN, respectively.

corresponding mesoporous property.[25,26] The apparent morphology difference suggests that water filled up the mesopores channel together with dissolved cyanamide precursor in the liquid infiltration method might play an important role in determining the final morphologies of the carbon nitride samples. The corresponding SEM images of control samples (including mesoporous CN and bulky CN) were shown in Figure S7 of the Supporting Information.

The chemical valence state of the elements in CNR was checked by X-ray photoelectron spectroscopy (XPS). As displayed in Figure S8 in the Supporting Information, the survey XPS spectra of carbon nitride materials (including CNR, mesoporous CN, and bulky CN) contain only C, N, and O elements. Further high-resolution analysis demonstrates that the binding energies for C 1s and N 1s are exactly the same for all three different geometrical materials with the same carbon nitride composition. The Fourier transform infrared spectroscopy (FTIR) and powder X-ray diffraction (XRD) characterizations depicted in Figure 3 demonstrate the obtained CNR is a typical polymeric graphitic carbon nitride material. The band at 810 cm^{-1} in the FTIR spectra in Figure 3a is ascribed to the breathing mode of the triazine units, while the fingerprint region between 1200 and 1620 cm^{-1} showing all the feature-distinctive stretch modes of aromatic CN heterocycles that is dominated by ν(C-NH-C) and ν(C=N) stretching vibrations. The wide-angle XRD pattern shows the two characteristic peaks of graphitic carbon nitride (Figure 3b) at 13.0 and 27.4°. The dominating characteristic (002) peak centered at 27.4° features the layered structure with an interlayer distance of d = 0.326 nm. Another pronounced peak is found at 13.0°, which corresponds to an in-plane structural packing motif.

Figure 4a shows the optical properties of CNR, bulky carbon nitride (bulky CN), and mesoporous carbon nitride (mesorporous CN) as measured by UV–vis diffuse reflection spectra. The absorption cutoff wavelength of CNR is about 460 nm corresponding to a band gap energy of ~2.7 eV, indicating that the polymeric semiconductor absorbs the blue section of the visible spectrum. The photogenerated charge carrier separation and recombination were also investigated by photoluminescence spectra under excitation at 380 nm. As shown in Figure 4b, the CNR sample exhibits an extremely broad emission peak. Compared with the bulky CN, the red-shifted fluorescence emission peak of CNR is also greatly decreased, suggesting a suppressed recombination of the photoinduced charge carriers, which is beneficial for further heterogeneous photocatalysis. The broad red-shifted fluorescence peak can be attributed to

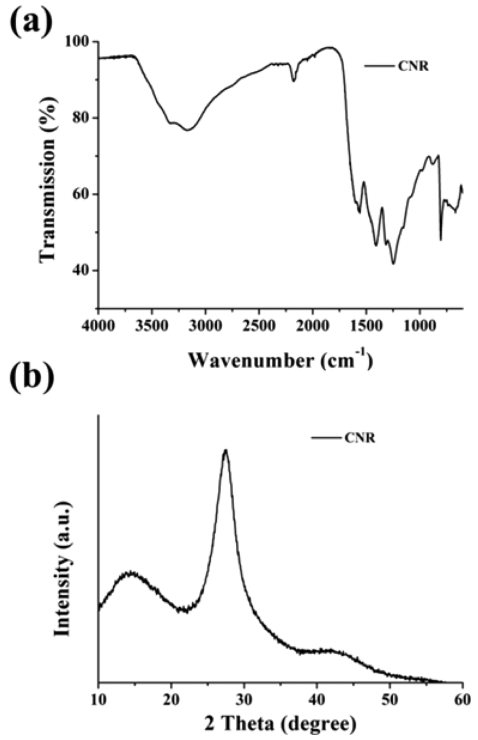

Figure 3. (a) FTIR spectrum of CNA showing typical C−N heterocycle stretches in the 1100−1600 cm^{-1} spectral range and the breathing mode of the tri-s-triazine units at 810 cm^{-1}. (b) XRD spectrum of CNA with two peaks at 13.0 and 27.4° ascribed to the in-planar repeat period and stacking of the conjugated aromatic system, respectively.

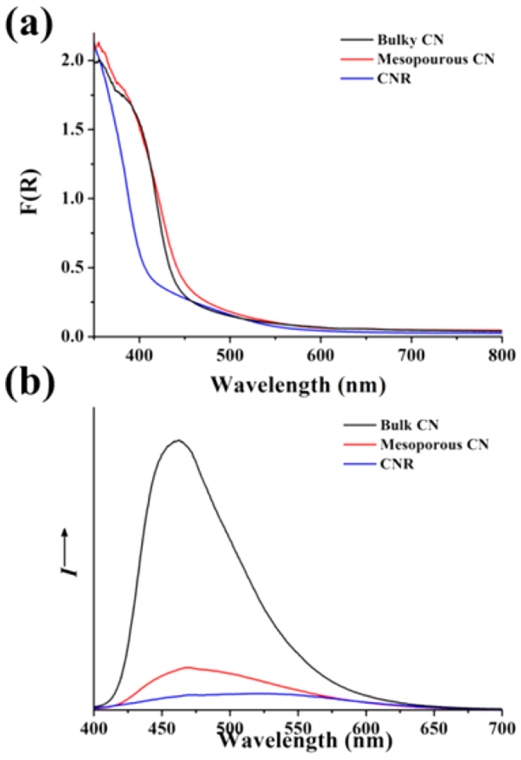

Figure 4. (a) Optical absorption and (b) photoluminescence spectra of CNR, mesoporous CN, and bulky CN samples, respectively.

the large amount of defect structures, which introduced localized energy levels inside the band gap.[27] The time-resolved PL experiments (as illustrated Figure S9 in the Supporting Information) detecting the recombination kinetics of photo-induced charge revealed that the fluorescence lifetime of CNR is 6.8 ns, slightly shorter than that of bulky one (~9 ns). This is due to an increased nonradiative rate, which follows an inverse trend with the fluorescence emission. The quenching of the emission intensity and its lifetime indicate that the relaxation of a fraction of carbon nitride excitons occurs via nonradiative paths, presumably by charge transfer of electrons and holes to new localized states, which were attributed to the introduction of nanostructures.

The photoelectrochemical behaviors of CNR accompanying with two control samples (bulky CN and mesoporous CN) were investigated by electrochemical impedance spectroscopy (Figure 5a). The results showed semicircular Nyquist plots for CNR, mesoporous CN and bulky CN with the trend of increasing diameter, demonstrating that CNR possessed a superior electronic conductivity compared with other morphologies. The photocurrent measurement was employed to illustrate photoinduced electron transfer processes occurred on carbon nitride materials casted on indium tin oxide glass (Figure 5b). Large enhancement of I_{ph} for CNR was indeed observed over the applied bias potential of 0.2 V versus Ag/AgCl, indicating faster transport of charged carriers. Carbon nitride materials were then evaluated in a photocatalytic hydrogen evolution activity test by loading 3 wt % Pt as cocatalyst and using triethanolamine as a hole scavenger. The hydrogen evolution results are presented in Figure 5c and Figure S10 in the Supporting Information. The performance of CNR in photocatalytic water splitting into hydrogen is much better than that of mesoporous CN, which usually serves as the benchmark for the carbon nitride based materials. The substantial enhancement should be ascribed to higher charge separation efficiency in the two-dimensional layered structures of CNR.

NADH, the biological form of hydrogen, is a coenzyme found in all living system. The pyridine nucleotides, NAD^+ (nicotinamide adenine dinucleotide) and NADP (nicotinamide adenine dinucleotide phosphate), are ubiquitous in all living systems as they are required for the reactions of more than 400 oxidoreductase-denoted dehydrogenases.[28] In metabolism, NADH/NAD^+ is involved in redox reactions, carrying electrons from one reaction to another. Maintaining the complete cycle between NAD^+ and NADH is extremely important for the dehydrogenase enzymatic reactions.[6,18] In light of the success of applying CNR in hydrogen evolution from water, the NADH regeneration was also performed by CNR photocatalysis with $[Cp^*Rh(bpy)(H)]^+$ acting as electron mediator and hydride transfer agent.[29] Under white light illumination, NADH regeneration yields for CNR and Mesoporous CN get to 72 and 65% in an hour, respectively (as illustrated in Figure S11 in the Supporting Information). The blank reactions without CNR or $[Cp^*Rh(bpy)(H)]^+$ were performed as illustrated in Figure S12 in the Supporting Information. Without CNR, the NADH cannot be regenerated in the same light illumination period; however, without $[Cp^*Rh(bpy)(H)]^+$, NADH can be moderately regenerated, but not all the regenerated NADH by metal-free method is enzymatically active.[15]

In the biosynthesis of amino acids, the first reaction of fundamental importance is biosynthesis of glutamate, from which other amino acids are synthesized.[30] The NADH

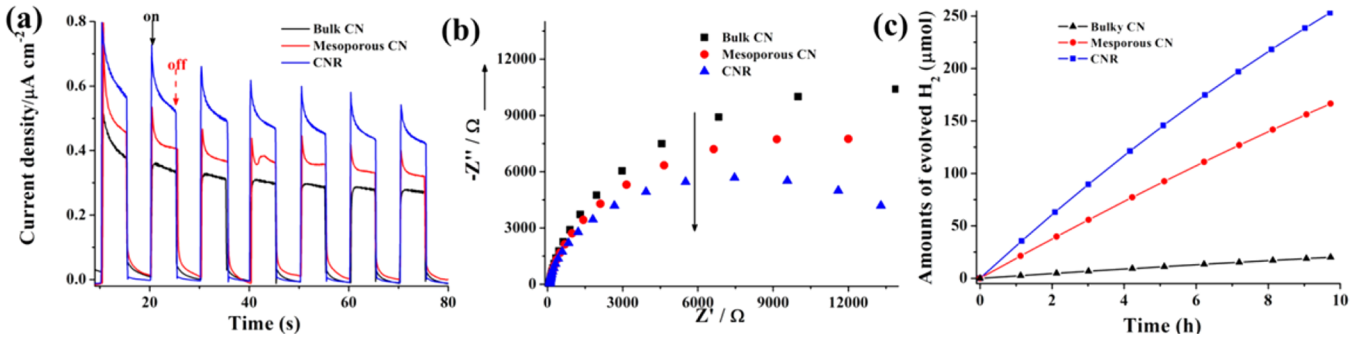

Figure 5. (a) Periodic on/off photocurrent output of CNR, mesoporous CN, and bulky CN casted on ITO glass at 0.2 V bias vs Ag/AgCl in a 0.2 M Na_2SO_4 solution. (b) Electrochemical impedance spectroscopy Nyquist plots for CNR, mesoporous CN, and bulky CN, respectively. (c) Time courses of H_2 evolution rate for CNR, mesoporous CN, and bulky CN during a 10 h experiment, respectively.

Scheme 1. Schematic Illustration of Photocatalytic NADH Regeneration by CNR in the Presence of $[Cp^*Rh(bpy)(H)]^+$ Acting As Electron Mediator and Hydride Transfer Agent; Regeneration of Catalytically Active $[Cp^*Rh(bpy)(H)]^+$ Is Also Illustrated

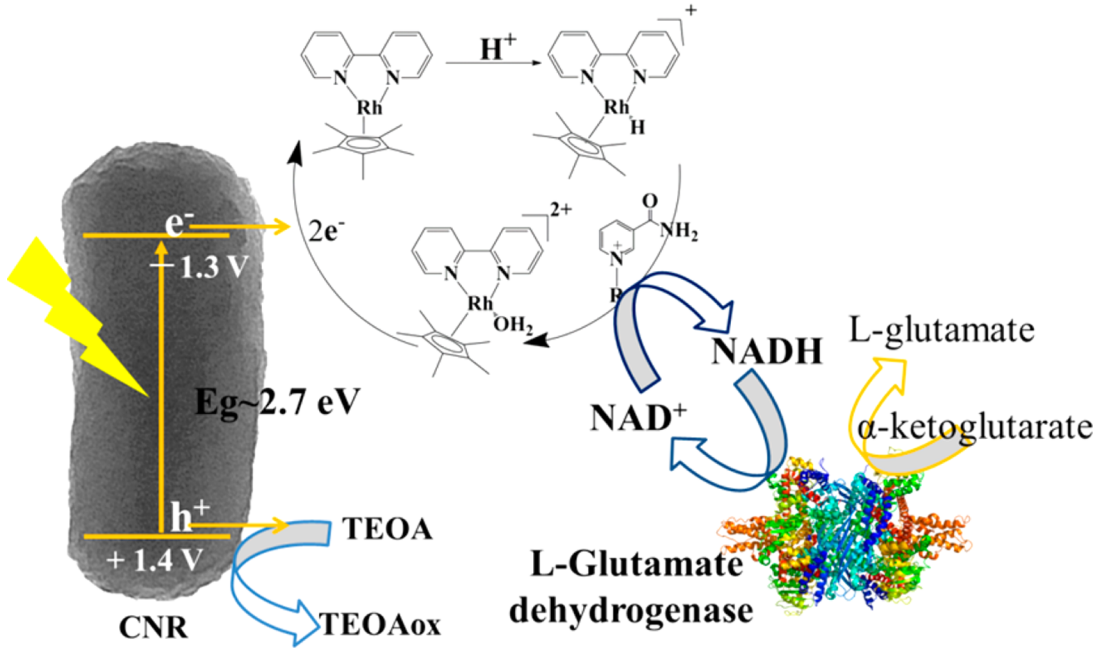

dependent L-glutamate dehydrogenase is capable for efficient biosynthesis of L-glutamate. Considering the previously reported coenzyme regeneration routes, using light to regenerate NADH for synthesizing L-glutamate will be sustainable and feasible.[18] A subsequent experiment was conducted to investigate whether CNR photocatalysis induces the reduction of NAD^+ to NADH followed by the biosynthesis of glutamate in the presence of L-glutamate dehydrogenase, as shown in Scheme 1.

The stoichiometry conversion of α-ketoglutarate to L-glutamate was accomplished after 8 h continuous light illumination, as illustrated in Figure 6. During the light reaction, the in situ regenerated NADH was immediately consumed by L-glutamate dehydrogenase for the synthesis of L-glutamate from α-ketoglutarate, whereas the NAD^+ could be repeatedly regenerated (The molar ratio of α-ketoglutarate to NAD^+ was chosen to be 10, indicating the NADH must be continuously regenerated for accomplishing the stoichiometric conversion). The yield was determined by the integration of NMR signals of the starting and ending reaction solutions, as shown in Figure S13 in the Supporting Information. Complete conversion of α-ketoglutarate to L-glutamate could be verified by the NMR spectra. However, in the dark without light irradiation, there is no L-glutamate product detected in the first hour. Therefore, it was feasible to synthesize L-glutamate from α-ketoglutarate assisting by L-glutamate dehydrogenase with CNR photocatalytic NADH regeneration system. This also represents the possibility for accomplishing the synthesis of even more complicated biomolecules starting from L-glutamate.[31−34]

CONCLUSIONS

In conclusion, uniform graphitic carbon nitride nanorod was easily obtained by a morphology-preserving strategy by facilely templating a chiral mesostructured silica nanorod. The one-dimensional hexagonal mesostructured pore structures of silica nanorod can provide nanoconfinement space for carbon nitride condensation to perfect layered structures. Because of the well-preserved layer properties, CNR demonstrated excellent photocatalytic capability in generating hydrogen from water even with small specific surface area, compared with mesoporous counterpart. For further demonstration, the

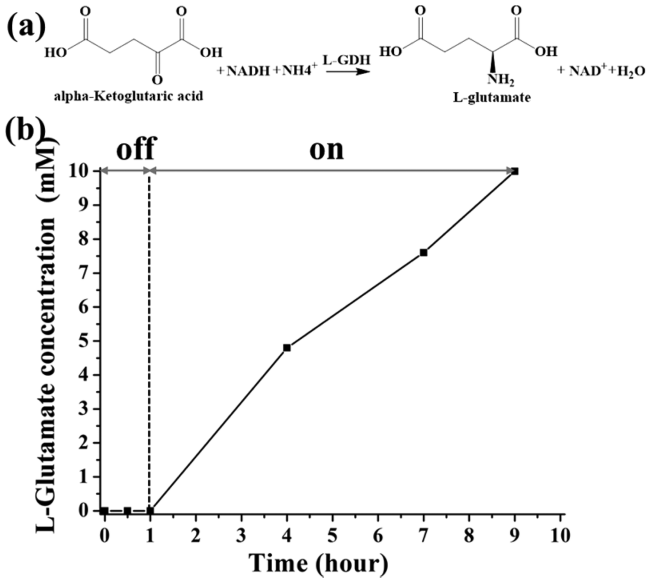

Figure 6. (a) Conversion between α-ketoglutarate and L-glutamate by L-glutamate dehydrogenase. (b) Photocatalytic propelled enzymatic synthesis of L-glutamate by CNR in the presence of M assisted by L-glutamate dehydrogenase. The reaction solution was first placed in the dark for 1 h before turn on the illumination.

CNR was used for photocatalytic regeneration of NADH from NAD^+. The in situ NADH regeneration system was coupled with L-glutamate dehydrogenase for sustainable synthesis of chiral L-glutamate from α-ketoglutarate. The facile synthesis of high efficiency CNR photocatalyst obtained here point a high-throughput way for practical enzymatic applications in the future. Practical artificial photosynthesis device could also be obtained by engineering the nanorod assembly into periodic and ordered array toward potential application in the near future.

■ ASSOCIATED CONTENT

Supporting Information

SEM, TEM, TGA, time-resolved PL and XPS of CNR, histogram of H_2 production capability, NADH spectral measurement, H NMR spectra of L-glutamate. This material is available free of charge via the Internet at http://pubs.acs.org.

■ AUTHOR INFORMATION

Corresponding Authors

*E-mail: Jian.Liu@mpikg.mpg.de.
*E-mail: owenhuang95@163.com.

Author Contributions

The manuscript was written through contributions of all authors. All authors have given approval to the final version of the manuscript.

Notes

The authors declare no competing financial interest.

■ ACKNOWLEDGMENTS

J.L. acknowledges the support of Alexander von Humboldt Foundation. J.H. acknowledges the support from National Natural Science Foundation of China (21103095) and the Excellent Young Scientific Research Talents in University of Fujian, China (JA12285). H.Z. acknowledges the financial support by the National Natural Science Foundation of China (51102163).

■ REFERENCES

(1) Barber, J. Photosynthetic Energy Conversion: Natural and Artificial. *Chem. Soc. Rev.* **2008**, *38*, 185−196.
(2) Han, Z.; Qiu, F.; Eisenberg, R.; Holland, P. L.; Krauss, T. D. Robust Photogeneration of H_2 in Water Using Semiconductor Nanocrystals and a Nickel Catalyst. *Science* **2012**, *338*, 1321−1324.
(3) Zhou, H.; Guo, J.; Li, P.; Fan, T.; Zhang, D.; Ye, J. Leaf-architectured 3D Hierarchical Artificial Photosynthetic System of Perovskite Titanates Towards CO_2 Photoreduction Into Hydrocarbon Fuels. *Sci. Rep.* **2013**, *3*, 1667.
(4) Mifsud, M.; Gargiulo, S.; Iborra, S.; Arends, I. W.; Hollmann, F.; Corma, A. Photobiocatalytic Chemistry of Oxidoreductases Using Water as the Electron Donor. *Nat. Commun.* **2014**, *5*, 3145.
(5) Gust, D.; Moore, T. A.; Moore, A. L. Solar Fuels via Artificial Photosynthesis. *Acc. Chem. Res.* **2009**, *42*, 1890−1898.
(6) Jianhui, Huang; Markus, Antonietti; Jian, Liu. Bio-inspired Carbon Nitride Mesoporous Spheres for Artificial Photosynthesis: Photocatalytic Cofactor Regeneration for Sustainable Enzymatic Synthesis. *J. Mater. Chem. A* **2014**, DOI: 10.1039 /C4TA00793J.
(7) Wang, F.; Wang, W. G.; Wang, X. J.; Wang, H. Y.; Tung, C. H.; Wu, L. Z. A Highly Efficient Photocatalytic System for Hydrogen Production by a Robust Hydrogenase Mimic in an Aqueous Solution. *Angew. Chem., Int. Ed.* **2011**, *50*, 3193−3197.
(8) Wang, X.; Maeda, K.; Thomas, A.; Takanabe, K.; Xin, G.; Carlsson, J. M.; Domen, K.; Antonietti, M. A Metal-free Polymeric Photocatalyst for Hydrogen Production from Water under Visible Light. *Nat. Mater.* **2008**, *8*, 76−80.
(9) Thomas, A.; Fischer, A.; Goettmann, F.; Antonietti, M.; Müller, J.-O.; Schlögl, R.; Carlsson, J. M. Graphitic Carbon Nitride Materials: Variation of Structure and Morphology and Their Use as Metal-free Catalysts. *J. Mater. Chem.* **2008**, *18*, 4893−4908.
(10) Wang, Y.; Wang, X.; Antonietti, M. Polymeric Graphitic Carbon Nitride as a Heterogeneous Organocatalyst: From Photochemistry to Multipurpose Catalysis to Sustainable Chemistry. *Angew. Chem., Int. Ed.* **2012**, *51*, 68−89.
(11) Zhang, J.; Wang, Y.; Jin, J.; Zhang, J.; Lin, Z.; Huang, F.; Yu, J. Efficient Visible-Light Photocatalytic Hydrogen Evolution and Enhanced Photostability of Core/Shell CdS/g-C_3N_4 Nanowires. *ACS Appl. Mater. Interfaces* **2013**, *5*, 10317−10324.
(12) Hou, Y.; Wen, Z.; Cui, S.; Guo, X.; Chen, J. Constructing 2D Porous Graphitic C_3N_4 Nanosheets/Nitrogen-Doped Graphene/Layered MoS_2 Ternary Nanojunction with Enhanced Photoelectrochemical Activity. *Adv. Mater.* **2013**, *25*, 6291−6297.
(13) Niu, P.; Zhang, L.; Liu, G.; Cheng, H. M. Graphene-Like Carbon Nitride Nanosheets for Improved Photocatalytic Activities. *Adv. Funct. Mater.* **2012**, *22*, 4763−4770.
(14) Sun, J.; Zhang, J.; Zhang, M.; Antonietti, M.; Fu, X.; Wang, X. Bioinspired Hollow Semiconductor Nanospheres as Photosynthetic Nanoparticles. *Nat. Commun.* **2012**, 1139.
(15) Liu, J.; Antonietti, M. Bio-inspired NADH Regeneration by Carbon Nitride Photocatalysis Using Diatom Templates. *Energy Environ. Sci.* **2013**, *6*, 1486−1493.
(16) Li, X.-H.; Zhang, J.; Chen, X.; Fischer, A.; Thomas, A.; Antonietti, M.; Wang, X. Condensed Graphitic Carbon Nitride Nanorods by Nanoconfinement: Promotion of Crystallinity on Photocatalytic Conversion. *Chem. Mater.* **2011**, *23*, 4344−4348.
(17) Ye, J.; Zhang, H.; Yang, R.; Li, X.; Qi, L. Morphology-Controlled Synthesis of SnO_2 Nanotubes by Using 1D Silica Mesostructures as Sacrificial Templates and Their Applications in Lithium-Ion Batteries. *Small* **2010**, *6*, 296−306.
(18) Wichmann, R.; Vasic-Racki, D., Cofactor Regeneration at the Lab Scale. In *Technology Transfer in Biotechnology*; Springer: New York, 2005; pp 225−260.
(19) Wong, C.-H.; Whitesides, G. M. Enzyme-catalyzed Organic Synthesis: NAD(P)H Cofactor Regeneration by Using Glucose-6-

phosphate and the Glucose-5-phosphate Dehydrogenase from Leuconostoc Mesenteroides. *J. Am. Chem. Soc.* **1981**, *103*, 4890−4899.
(20) Oppelt, K. T.; Wöß, E.; Stiftinger, M.; Schöfberger, W.; Buchberger, W.; Knör, G. n. Photocatalytic Reduction of Artificial and Natural Nucleotide Co-factors with a Chlorophyll-Like Tin-Dihydroporphyrin Sensitizer. *Inorg. Chem.* **2013**, *52*, 11910−11922.
(21) Ryu, J.; Lee, S. H.; Nam, D. H.; Park, C. B. Rational Design and Engineering of Quantum-Dot-Sensitized TiO_2 Nanotube Arrays for Artificial Photosynthesis. *Adv. Mater.* **2011**, *23*, 1883−1888.
(22) Asada, H.; Itoh, T.; Kodera, Y.; Matsushima, A.; Hiroto, M.; Nishimura, H.; Inada, Y. Glutamate Synthesis via Photoreduction of $NADP^+$ by Photostable Chlorophyllide Coupled with Polyethyleneglycol. *Biotechnol. Bioeng.* **2001**, *76*, 86−90.
(23) Yadav, R. K.; Baeg, J.-O.; Oh, G. H.; Park, N.-J.; Kong, K.-J.; Kim, J.; Hwang, D. W.; Biswas, S. K. A Photocatalyst-Enzyme Coupled Artificial Photosynthesis System for Solar Energy in Production of Formic Acid from CO_2. *J. Am. Chem. Soc.* **2012**, *134*, 11455−11461.
(24) Park, S. S.; Chu, S.-W.; Xue, C.; Zhao, D.; Ha, C.-S. Facile Synthesis of Mesoporous Carbon Nitrides Using the Incipient Wetness Method and the Application as Hydrogen Adsorbent. *J. Mater. Chem.* **2011**, *21*, 10801−10807.
(25) Li, X.-H.; Wang, X.; Antonietti, M. Mesoporous g-C_3N_4 Nanorods as Multifunctional Supports of Ultrafine Metal Nanoparticles: Hydrogen Generation from Water and Reduction of Nitrophenol with Tandem Catalysis in One Step. *Chemical Science* **2012**, *3*, 2170−2174.
(26) Chen, X.; Jun, Y.-S.; Takanabe, K.; Maeda, K.; Domen, K.; Fu, X.; Antonietti, M.; Wang, X. Ordered Mesoporous SBA-15 Type Graphitic Carbon Nitride: A Semiconductor Host Structure for Photocatalytic Hydrogen Evolution with Visible Light. *Chem. Mater.* **2009**, *21*, 4093−4095.
(27) Bai, X.; Wang, L.; Zong, R.; Zhu, Y. Photocatalytic Activity Enhanced via g-C_3N_4 Nanoplates to Nanorods. *J. Phys. Chem. C* **2013**, *117*, 9952−9961.
(28) Gorton, L.; Domínguez, E. Electrochemistry of $NAD(P)^+$/NAD(P)H. In *Encyclopedia of Electrochemistry*; Wiley: New York, 2002.
(29) Hollmann, F.; Witholt, B.; Schmid, A. $[Cp^*Rh(bpy)(H_2O)]^{2+}$: A Versatile Tool for Efficient and Non-enzymatic Regeneration of Nicotinamide and Flavin Coenzymes. *J. Mol. Catal. B: Enzym.* **2002**, *19*, 167−176.
(30) Nelson, D. L.; Lehninger, A. L.; Cox, M. M. *Lehninger Principles of Biochemistry*; Macmillan: London, 2008.
(31) Könst, P.; Merkens, H.; Kara, S.; Kochius, S.; Vogel, A.; Zuhse, R.; Holtmann, D.; Arends, I. W.; Hollmann, F. Enantioselective Oxidation of Aldehydes Catalyzed by Alcohol Dehydrogenase. *Angew. Chem., Int. Ed.* **2012**, *51*, 9914−9917.
(32) Lo, H. C.; Fish, R. H. Biomimetic NAD^+ Models for Tandem Cofactor Regeneration, Horse Liver Alcohol Dehydrogenase Recognition of 1, 4-NADH Derivatives, and Chiral Synthesis. *Angew. Chem., Int. Ed.* **2002**, *41*, 478−481.
(33) Choudhury, S.; Baeg, J. O.; Park, N. J.; Yadav, R. K. A Photocatalyst/Enzyme Couple That Uses Solar Energy in the Asymmetric Reduction of Acetophenones. *Angew. Chem., Int. Ed.* **2012**, *124*, 11792−11796.
(34) Chenault, H. K.; Whitesides, G. M. Regeneration of Nicotinamide Cofactors for Use in Organic Synthesis. *Appl. Bochem. Biotechnol.* **1987**, *14*, 147−197.